Study of $B^0 \to J/\psi K^{(*)0}\pi^+\pi^-$ Decays with the Collider Detector at Fermilab

T. Affolder,[1] H. Akimoto,[2] A. Akopian,[3] M. G. Albrow,[4] P. Amaral,[5] D. Amidei,[6] K. Anikeev,[7] J. Antos,[8] G. Apollinari,[4] T. Arisawa,[2] A. Artikov,[9] T. Asakawa,[10] W. Ashmanskas,[5] F. Azfar,[11] P. Azzi-Bacchetta,[12] N. Bacchetta,[12] H. Bachacou,[1] S. Bailey,[13] P. de Barbaro,[14] A. Barbaro-Galtieri,[1] V. E. Barnes,[15] B. A. Barnett,[16] S. Baroiant,[17] M. Barone,[18] G. Bauer,[7] F. Bedeschi,[19] S. Belforte,[20] W. H. Bell,[21] G. Bellettini,[19] J. Bellinger,[22] D. Benjamin,[23] J. Bensinger,[24] A. Beretvas,[4] J. P. Berge,[4] J. Berryhill,[5] A. Bhatti,[3] M. Binkley,[4] D. Bisello,[12] M. Bishai,[4] R. E. Blair,[25] C. Blocker,[24] K. Bloom,[6] B. Blumenfeld,[16] S. R. Blusk,[14] A. Bocci,[3] A. Bodek,[14] W. Bokhari,[26] G. Bolla,[15] Y. Bonushkin,[27] D. Bortoletto,[15] J. Boudreau,[28] A. Brandl,[29] S. van den Brink,[16] C. Bromberg,[30] M. Brozovic,[23] E. Brubaker,[1] N. Bruner,[29] E. Buckley-Geer,[4] J. Budagov,[9] H. S. Budd,[14] K. Burkett,[13] G. Busetto,[12] A. Byon-Wagner,[4] K. L. Byrum,[25] S. Cabrera,[23] P. Calafiura,[1] M. Campbell,[6] W. Carithers,[1] J. Carlson,[6] D. Carlsmith,[22] W. Caskey,[17] A. Castro,[31] D. Cauz,[20] A. Cerri,[19] A. W. Chan,[8] P. S. Chang,[8] P. T. Chang,[8] J. Chapman,[6] C. Chen,[26] Y. C. Chen,[8] M.-T. Cheng,[8] M. Chertok,[17] G. Chiarelli,[19] I. Chirikov-Zorin,[9] G. Chlachidze,[9] F. Chlebana,[4] L. Christofek,[32] M. L. Chu,[8] Y. S. Chung,[14] C. I. Ciobanu,[33] A. G. Clark,[34] A. P. Colijn,[4] A. Connolly,[1] J. Conway,[35] M. Cordelli,[18] J. Cranshaw,[36] R. Cropp,[37] R. Culbertson,[4] D. Dagenhart,[38] S. D'Auria,[21] F. DeJongh,[4] S. Dell'Agnello,[18] M. Dell'Orso,[19] L. Demortier,[3] M. Deninno,[31] P. F. Derwent,[4] T. Devlin,[35] J. R. Dittmann,[4] A. Dominguez,[1] S. Donati,[19] J. Done,[39] M. D'Onofrio,[19] T. Dorigo,[13] N. Eddy,[32] K. Einsweiler,[1] J. E. Elias,[4] E. Engels, Jr.,[28] R. Erbacher,[4] D. Errede,[32] S. Errede,[32] Q. Fan,[14] H.-C. Fang,[1] R. G. Feild,[40] J. P. Fernandez,[4] C. Ferretti,[19] R. D. Field,[41] I. Fiori,[31] B. Flaugher,[4] G. W. Foster,[4] M. Franklin,[13] J. Freeman,[4] J. Friedman,[7] Y. Fukui,[42] I. Furic,[7] S. Galeotti,[19] A. Gallas,[13,*] M. Gallinaro,[3] T. Gao,[26] M. Garcia-Sciveres,[1] A. F. Garfinkel,[15] P. Gatti,[12] C. Gay,[40] D. W. Gerdes,[6] P. Giannetti,[19] P. Giromini,[18] V. Glagolev,[9] D. Glenzinski,[4] M. Gold,[29] J. Goldstein,[4] I. Gorelov,[29] A. T. Goshaw,[23] Y. Gotra,[28] K. Goulianos,[3] C. Green,[15] G. Grim,[17] P. Gris,[4] L. Groer,[35] C. Grosso-Pilcher,[5] M. Guenther,[15] G. Guillian,[6] J. Guimaraes da Costa,[13] R. M. Haas,[41] C. Haber,[1] S. R. Hahn,[4] C. Hall,[13] T. Handa,[43] R. Handler,[22] W. Hao,[36] F. Happacher,[18] K. Hara,[10] A. D. Hardman,[15] R. M. Harris,[4] F. Hartmann,[44] K. Hatakeyama,[3] J. Hauser,[27] J. Heinrich,[26] A. Heiss,[44] M. Herndon,[16] C. Hill,[17] K. D. Hoffman,[15] C. Holck,[26] R. Hollebeek,[26] L. Holloway,[32] B. T. Huffman,[11] R. Hughes,[33] J. Huston,[30] J. Huth,[13] H. Ikeda,[10] J. Incandela,[4,†] G. Introzzi,[19] J. Iwai,[2] Y. Iwata,[43] E. James,[6] M. Jones,[26] U. Joshi,[4] H. Kambara,[34] T. Kamon,[39] T. Kaneko,[10] K. Karr,[38] H. Kasha,[40] Y. Kato,[45] T. A. Keaffaber,[15] K. Kelley,[7] M. Kelly,[6] R. D. Kennedy,[4] R. Kephart,[4] D. Khazins,[23] T. Kikuchi,[10] B. Kilminster,[14] B. J. Kim,[46] D. H. Kim,[46] H. S. Kim,[32] M. J. Kim,[46] S. B. Kim,[46] S. H. Kim,[10] Y. K. Kim,[1] M. Kirby,[23] M. Kirk,[24] L. Kirsch,[24] S. Klimenko,[41] P. Koehn,[33] K. Kondo,[2] J. Konigsberg,[41] A. Korn,[7] A. Korytov,[41] E. Kovacs,[25] J. Kroll,[26] M. Kruse,[23] S. E. Kuhlmann,[25] K. Kurino,[43] T. Kuwabara,[10] A. T. Laasanen,[15] N. Lai,[5] S. Lami,[3] S. Lammel,[4] J. Lancaster,[23] M. Lancaster,[1] R. Lander,[17] A. Lath,[35] G. Latino,[19] T. LeCompte,[25] A. M. Lee IV,[23] K. Lee,[36] S. Leone,[19] J. D. Lewis,[4] M. Lindgren,[27] T. M. Liss,[32] J. B. Liu,[14] Y. C. Liu,[8] D. O. Litvintsev,[4] O. Lobban,[36] N. Lockyer,[26] J. Loken,[11] M. Loreti,[12] D. Lucchesi,[12] P. Lukens,[4] S. Lusin,[22] L. Lyons,[11] J. Lys,[1] R. Madrak,[13] K. Maeshima,[4] P. Maksimovic,[13] L. Malferrari,[31] M. Mangano,[19] M. Mariotti,[12] G. Martignon,[12] A. Martin,[40] J. A. J. Matthews,[29] J. Mayer,[37] P. Mazzanti,[31] K. S. McFarland,[14] P. McIntyre,[39] E. McKigney,[26] M. Menguzzato,[12] A. Menzione,[19] P. Merkel,[4] C. Mesropian,[3] A. Meyer,[4] T. Miao,[4] R. Miller,[30] J. S. Miller,[6] H. Minato,[10] S. Miscetti,[18] M. Mishina,[42] G. Mitselmakher,[41] N. Moggi,[31] E. Moore,[29] R. Moore,[6] Y. Morita,[42] T. Moulik,[15] M. Mulhearn,[7] A. Mukherjee,[4] T. Muller,[44] A. Munar,[19] P. Murat,[4] S. Murgia,[30] J. Nachtman,[27] V. Nagaslaev,[36] S. Nahn,[40] H. Nakada,[10] I. Nakano,[43] C. Nelson,[4] T. Nelson,[4] C. Neu,[33] D. Neuberger,[44] C. Newman-Holmes,[4] C.-Y. P. Ngan,[7] H. Niu,[24] L. Nodulman,[25] A. Nomerotski,[41] S. H. Oh,[23] Y. D. Oh,[46] T. Ohmoto,[43] T. Ohsugi,[43] R. Oishi,[10] T. Okusawa,[45] J. Olsen,[22] W. Orejudos,[1] C. Pagliarone,[19] F. Palmonari,[19] R. Paoletti,[19] V. Papadimitriou,[36] D. Partos,[24] J. Patrick,[4] G. Pauletta,[20] M. Paulini,[1,‡] C. Paus,[7] D. Pellett,[17] L. Pescara,[12] T. J. Phillips,[23] G. Piacentino,[19] K. T. Pitts,[32] A. Pompos,[15] L. Pondrom,[22] G. Pope,[28] M. Popovic,[37] F. Prokoshin,[9] J. Proudfoot,[25] F. Ptohos,[18] O. Pukhov,[9] G. Punzi,[19] A. Rakitine,[7] F. Ratnikov,[35] D. Reher,[1] A. Reichold,[11] A. Ribon,[12] W. Riegler,[13] F. Rimondi,[31] L. Ristori,[19] M. Riveline,[37] W. J. Robertson,[23] A. Robinson,[37] T. Rodrigo,[47] S. Rolli,[38] L. Rosenson,[7] R. Roser,[4] R. Rossin,[12] C. Rott,[15] A. Roy,[15] A. Ruiz,[47] A. Safonov,[17] R. St. Denis,[21] W. K. Sakumoto,[14] D. Saltzberg,[27] C. Sanchez,[33] A. Sansoni,[18] L. Santi,[20] H. Sato,[10] P. Savard,[37] P. Schlabach,[4] E. E. Schmidt,[4] M. P. Schmidt,[40] M. Schmitt,[13,*] L. Scodellaro,[12] A. Scott,[27] A. Scribano,[19] S. Segler,[4] S. Seidel,[29] Y. Seiya,[10] A. Semenov,[9] F. Semeria,[31] T. Shah,[7] M. D. Shapiro,[1] P. F. Shepard,[28] T. Shibayama,[10] M. Shimojima,[10] M. Shochet,[5] A. Sidoti,[12] J. Siegrist,[1] A. Sill,[36]

 0031-9007/02/88(7)/071801(6)$20.00

P. Sinervo,[37] P. Singh,[32] A. J. Slaughter,[40] K. Sliwa,[38] C. Smith,[16] F. D. Snider,[4] A. Solodsky,[3] J. Spalding,[4] T. Speer,[34] P. Sphicas,[7] F. Spinella,[19] M. Spiropulu,[13] L. Spiegel,[4] J. Steele,[22] A. Stefanini,[19] J. Strologas,[32] F. Strumia,[34] D. Stuart,[4] K. Sumorok,[7] T. Suzuki,[10] T. Takano,[45] R. Takashima,[43] K. Takikawa,[10] P. Tamburello,[23] M. Tanaka,[10] B. Tannenbaum,[27] M. Tecchio,[6] R. Tesarek,[4] P. K. Teng,[8] K. Terashi,[3] S. Tether,[7] A. S. Thompson,[21] R. Thurman-Keup,[25] P. Tipton,[14] S. Tkaczyk,[4] D. Toback,[39] K. Tollefson,[14] A. Tollestrup,[4] D. Tonelli,[19] H. Toyoda,[45] W. Trischuk,[37] J. F. de Troconiz,[13] J. Tseng,[7] N. Turini,[19] F. Ukegawa,[10] T. Vaiciulis,[14] J. Valls,[35] S. Vejcik III,[4] G. Velev,[4] G. Veramendi,[1] R. Vidal,[4] I. Vila,[47] R. Vilar,[47] I. Volobouev,[1] M. von der Mey,[27] D. Vucinic,[7] R. G. Wagner,[25] R. L. Wagner,[4] N. B. Wallace,[35] Z. Wan,[35] C. Wang,[23] M. J. Wang,[8] B. Ward,[21] S. Waschke,[21] T. Watanabe,[10] D. Waters,[11] T. Watts,[35] R. Webb,[39] H. Wenzel,[44] W. C. Wester III,[4] A. B. Wicklund,[25] E. Wicklund,[4] T. Wilkes,[17] H. H. Williams,[26] P. Wilson,[4] B. L. Winer,[33] D. Winn,[6] S. Wolbers,[4] D. Wolinski,[6] J. Wolinski,[30] S. Wolinski,[6] S. Worm,[29] X. Wu,[34] J. Wyss,[19] W. Yao,[1] G. P. Yeh,[4] P. Yeh,[8] J. Yoh,[4] C. Yosef,[30] T. Yoshida,[45] I. Yu,[46] S. Yu,[26] Z. Yu,[40] A. Zanetti,[20] F. Zetti,[1] and S. Zucchelli[31]

(CDF Collaboration)

[1]*Ernest Orlando Lawrence Berkeley National Laboratory, Berkeley, California 94720*
[2]*Waseda University, Tokyo 169, Japan*
[3]*Rockefeller University, New York, New York 10021*
[4]*Fermi National Accelerator Laboratory, Batavia, Illinois 60510*
[5]*Enrico Fermi Institute, University of Chicago, Chicago, Illinois 60637*
[6]*University of Michigan, Ann Arbor, Michigan 48109*
[7]*Massachusetts Institute of Technology, Cambridge, Massachusetts 02139*
[8]*Institute of Physics, Academia Sinica, Taipei, Taiwan 11529, Republic of China*
[9]*Joint Institute for Nuclear Research, RU-141980 Dubna, Russia*
[10]*University of Tsukuba, Tsukuba, Ibaraki 305, Japan*
[11]*University of Oxford, Oxford OX1 3RH, United Kingdom*
[12]*Universita di Padova, Istituto Nazionale di Fisica Nucleare, Sezione di Padova, I-35131 Padova, Italy*
[13]*Harvard University, Cambridge, Massachusetts 02138*
[14]*University of Rochester, Rochester, New York 14627*
[15]*Purdue University, West Lafayette, Indiana 47907*
[16]*The Johns Hopkins University, Baltimore, Maryland 21218*
[17]*University of California at Davis, Davis, California 95616*
[18]*Laboratori Nazionali di Frascati, Istituto Nazionale di Fisica Nucleare, I-00044 Frascati, Italy*
[19]*Istituto Nazionale di Fisica Nucleare, University and Scuola Normale Superiore of Pisa, I-56100 Pisa, Italy*
[20]*Istituto Nazionale di Fisica Nucleare, University of Trieste/Udine, Italy*
[21]*Glasgow University, Glasgow G12 8QQ, United Kingdom*
[22]*University of Wisconsin, Madison, Wisconsin 53706*
[23]*Duke University, Durham, North Carolina 27708*
[24]*Brandeis University, Waltham, Massachusetts 02254*
[25]*Argonne National Laboratory, Argonne, Illinois 60439*
[26]*University of Pennsylvania, Philadelphia, Pennsylvania 19104*
[27]*University of California at Los Angeles, Los Angeles, California 90024*
[28]*University of Pittsburgh, Pittsburgh, Pennsylvania 15260*
[29]*University of New Mexico, Albuquerque, New Mexico 87131*
[30]*Michigan State University, East Lansing, Michigan 48824*
[31]*Istituto Nazionale di Fisica Nucleare, University of Bologna, I-40127 Bologna, Italy*
[32]*University of Illinois, Urbana, Illinois 61801*
[33]*The Ohio State University, Columbus, Ohio 43210*
[34]*University of Geneva, CH-1211 Geneva 4, Switzerland*
[35]*Rutgers University, Piscataway, New Jersey 08855*
[36]*Texas Tech University, Lubbock, Texas 79409*
[37]*Institute of Particle Physics, University of Toronto, Toronto M5S 1A7, Canada*
[38]*Tufts University, Medford, Massachusetts 02155*
[39]*Texas A&M University, College Station, Texas 77843*
[40]*Yale University, New Haven, Connecticut 06520*
[41]*University of Florida, Gainesville, Florida 32611*
[42]*High Energy Accelerator Research Organization (KEK), Tsukuba, Ibaraki 305, Japan*
[43]*Hiroshima University, Higashi-Hiroshima 724, Japan*
[44]*Institut für Experimentelle Kernphysik, Universität Karlsruhe, 76128 Karlsruhe, Germany*

[45]Osaka City University, Osaka 588, Japan
[46]Center for High Energy Physics, Kyungpook National University, Taegu 702-701, Korea,
Seoul National University, Seoul 151-742, Korea,
and SungKyunKwan University, Suwon 440-746, Korea
[47]Instituto de Fisica de Cantabria, CSIC-University of Cantabria, 39005 Santander, Spain
(Received 31 July 2001; published 30 January 2002)

We report a study of the decays $B^0 \to J/\psi K^{(*)0}\pi^+\pi^-$, which involve the creation of a $u\bar{u}$ or $d\bar{d}$ quark pair in addition to a $\bar{b} \to \bar{c}(c\bar{s})$ decay. The data sample consists of 110 pb^{-1} of $p\bar{p}$ collisions at $\sqrt{s} =$ 1.8 TeV collected by the CDF detector at the Fermilab Tevatron collider during 1992–1995. We measure the branching fractions to be $\mathcal{B}(B^0 \to J/\psi K^{*0}\pi^+\pi^-) = (6.6 \pm 1.9 \pm 1.1) \times 10^{-4}$ and $\mathcal{B}(B^0 \to J/\psi K^0\pi^+\pi^-) = (10.3 \pm 3.3 \pm 1.5) \times 10^{-4}$. Evidence is seen for contributions from $\psi(2S)K^{(*)0}$, $J/\psi K^0\rho^0$, $J/\psi K^{*+}\pi^-$, and $J/\psi K_1(1270)$.

DOI: 10.1103/PhysRevLett.88.071801 PACS numbers: 13.25.Hw, 14.40.Nd

The measured inclusive branching fraction for $B \to J/\psi X$ of $(1.16 \pm 0.10)\%$ is considerably larger than the sum of the individual branching fractions of the known exclusively reconstructed decays [1]. One possible source of the missing decay modes is a class of decays in which a quark pair is created in addition to a $\bar{b} \to \bar{c}(c\bar{s})$ decay. The CLEO Collaboration recently reported observing one such mode, $B \to J/\psi\phi K$ [2], which involves an $s\bar{s}$ quark pair. This analysis studies similar B^0 decays that involve $u\bar{u}$ or $d\bar{d}$ quark pairs. These modes are potentially useful for CP violation measurements. For example, $J/\psi K^0_S\pi^+\pi^-$ is accessible from both B^0 and $\bar{B}^0$ which allows CP violation due to interference between decays with and without mixing. Since the final product is not a CP eigenstate, an angular analysis would be required to separate the CP-even and CP-odd contributions [3].

This analysis was performed using $p\bar{p}$ collisions recorded with the CDF detector, which is described in detail elsewhere [4]. For this analysis the important components are the Silicon Vertex Detector (SVX), the Central Tracking Chamber (CTC), and the central muon systems. The SVX provides a track impact parameter resolution of $\sim(13 + 40/p_T)$ μm, where p_T (in GeV/c) is the component of the momentum transverse to the $p\bar{p}$ collision axis (the z axis) [5]. The CTC is a drift chamber whose charged particle momentum resolution is $\delta p_T/p_T^2 \sim 0.001/(\mathrm{GeV}/c)$. Two muon systems separated by 60 cm of steel cover the region $|\eta| < 0.6$ for muons with $p_T >$ 1.4 GeV/c. Each of these central muon systems consists of four layers of planar drift chambers. The inner system is separated from the interaction point by an average of five interaction lengths of material. An extension to the central muon systems covers $0.6 < |\eta| < 1.0$.

This analysis uses a three-level dimuon trigger. The first level selects events with two separate sets of at least three linked hits in the muon chambers that cover $|\eta| < 1.0$. The second level requires drift chamber tracks with $p_T >$ 2.0 GeV/c which extrapolate to the linked hits in the muon chambers. The third level accepts $J/\psi \to \mu^+\mu^-$ candidates with a reconstructed invariant mass between 2.8 and 3.4 GeV/c^2. In addition to this trigger path, approximately 10% of the events which pass the level 3 dimuon trigger come from single muon triggers at levels 1 and 2 with muon p_T thresholds of either 7.5 or 12 GeV/c.

The off-line analysis reconstructs $J/\psi \to \mu^+\mu^-$ candidates but does not require them to be the same candidate which passed the trigger. The off-line reconstruction uses only muons which intersect both of the muon systems that cover $|\eta| < 0.6$.

A ratio of branching fractions is measured between a signal mode $B^0 \to J/\psi K^{(*)0}\pi^+\pi^-$ and a well established reference mode $B^0 \to J/\psi K^{(*)0}$ [1]:

$$\frac{\mathcal{B}_{\mathrm{sig}}}{\mathcal{B}_{\mathrm{ref}}} = \frac{\epsilon_{\mathrm{ref}}}{\epsilon_{\mathrm{sig}}} \frac{N_{\mathrm{sig}}}{N_{\mathrm{ref}}}. \quad (1)$$

Many systematic uncertainties cancel in this ratio. The ratio of efficiencies $R_\epsilon = \epsilon_{\mathrm{ref}}/\epsilon_{\mathrm{sig}}$ is determined with a Monte Carlo simulation. The number of signal and reference candidates (N_{sig} and N_{ref}) are measured in the data while applying similar selection criteria to both signal and reference decay modes. The only selection criteria which differ are those placed upon the two extra pions of the signal candidates for which there are no equivalents in the reference decays.

From the dimuon trigger events, B^0 decay candidates are selected which satisfy the basic topology of the decays of interest. The reference modes are reconstructed by combining a $J/\psi \to \mu^+\mu^-$ candidate with either a $K^0_S \to \pi^+\pi^-$ or $K^{*0} \to K^+\pi^-$ candidate. K^0_S candidates are required to have an invariant mass between 485 and 510 MeV/c^2 while constrained to point back to the J/ψ decay vertex. Additionally, the K^0_S candidates' decay vertices are required to have a positive displacement in the xy plane from the J/ψ decay vertex with at least 5σ significance. K^{*0} candidates are required to have an invariant mass between 820 and 970 MeV/c^2 and to originate from the J/ψ candidate decay vertex. To reduce backgrounds, all final state particles are required to have $p_T >$ 0.5 GeV/c, to be within $\Delta R \equiv \sqrt{\Delta\eta^2 + \Delta\phi^2} < 1.0$ of each other, and to originate within 5 cm of each other in z. The signal modes are reconstructed identically to

the reference modes, except for the addition of two pions which originate from the J/ψ candidate decay vertex. The invariant mass of these two extra pions, $m(\pi^+\pi^-)$, is required to be greater than 0.55 GeV/c^2.

The final vertex fit constrains the particles to originate from a common vertex, except the K^0_S daughters whose combined momentum must point back to that vertex. For this fit, the invariant masses of the K^0_S and J/ψ candidates are constrained to their world average measured values [1]. The χ^2 of the fit is required to have a confidence level above 0.1%.

If there are multiple B^0 decay candidates in the same event, all candidates are kept. Multiple candidates have the largest effect in the $B^0 \to J/\psi K^{*0}\pi^+\pi^-$ sample where misassignments of the K from the K^{*0} with other particles in the event result in a broad Gaussian shaped background. Multiple candidates do not significantly affect the $B^0 \to J/\psi K^0_S\pi^+\pi^-$ sample.

To reduce background levels, additional selection criteria are placed on the transverse momentum of the neutral kaon, $p_T(K^{(*)0})$, the proper decay time of the B^0 candidate, $ct(B)$, and a B^0 isolation variable, $I \equiv p_T(B)/[p_T(B) + p_T(x)]$. The quantity $p_T(x)$ is the scalar sum of the transverse momenta of all non-B^0 candidate tracks within $\Delta R < 1.0$ of the B^0 candidate momentum direction. For each signal mode these selection criteria are optimized to maximize $S^2/(S + Bkg)$ of the signal sample where S is the expected signal size and Bkg is the expected background size. This optimization uses the sidebands of the invariant mass distribution of the signal data and the invariant mass distribution of the reference data.

The optimized selection criteria for $B^0 \to J/\psi K^{*0}\pi^+\pi^-$ are $p_T(K^{*0}) > 2.4$ GeV/c, $ct(B) > 170$ μm, and $I > 0.60$. Figure 1(a) shows the resulting invariant mass peak. The data are fit using the sum of a narrow signal Gaussian, a broad background Gaussian, and a linear combinatoric background. The widths of the narrow and broad Gaussians are fixed to 11.8 and 145 MeV/c^2, respectively, based upon the expected width from the Monte Carlo simulation scaled up by the ratio of widths between the data and Monte Carlo simulation for the reference mode $B^0 \to J/\psi K^{*0}$. Their areas vary independently in the fit. The fit results in 36.3 ± 9.9 signal candidates with the broad Gaussian area consistent with expectations from Monte Carlo simulations. The $B^0 \to J/\psi K^{*0}$ reference mode with similar selection criteria has 257 ± 18 signal candidates. The ratio of reconstruction efficiencies between $B^0 \to J/\psi K^{*0}$ and $B^0 \to J/\psi K^{*0}\pi^+\pi^-$ is $R_\epsilon = 3.75$. These numbers lead to a ratio of branching fractions of $\mathcal{B}(B^0 \to J/\psi K^{*0}\pi^+\pi^-)/\mathcal{B}(B^0 \to J/\psi K^{*0}) = 0.53 \pm 0.15$, where the error is statistical only. Using $\mathcal{B}(B^0 \to J/\psi K^{*0}) = 12.4 \times 10^{-4}$ [6], this corresponds to a branching fraction of $\mathcal{B}(J/\psi K^{*0}\pi^+\pi^-) = (6.6 \pm 1.9) \times 10^{-4}$.

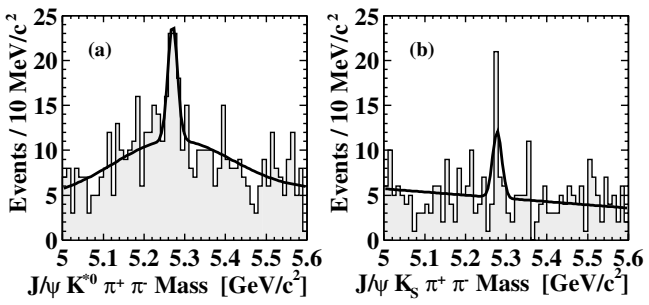

FIG. 1. Invariant masses of B^0 candidates for $B^0 \to J/\psi K^{*0}\pi^+\pi^-$ (a) and $B^0 \to J/\psi K^0_S\pi^+\pi^-$ (b).

The final state $J/\psi K^{*0}\pi^+\pi^-$ could come from the intermediate states $B^0 \to \psi(2S)K^{*0}$ or $B^0 \to J/\psi K^{*0}\rho^0$. Within $\pm 2\sigma$ of the B^0 invariant mass shown in Fig. 1(a), there are nine $\psi(2S) \to J/\psi\pi^+\pi^-$ candidates on an expected background of 3 within ± 10 MeV/c^2 of the $\psi(2S)$ mass of 3.686 GeV/c^2 [1]. The remaining signal candidates have higher $J/\psi\pi^+\pi^-$ invariant masses. There is no identifiable resonant structure in the $\pi^+\pi^-$ invariant mass distribution to indicate a large ρ^0 contribution, nor is there any identifiable resonant structure to the $K^{*0}\pi^\pm$ or $K^{*0}\pi^+\pi^-$ invariant mass distributions.

The identity of the K^{*0} was checked by broadening the $K^{*0} \to K\pi$ invariant mass selection. The $J/\psi K^{*0}\pi^+\pi^-$ background increased while the signal size did not, indicating a dominant K^{*0} contribution with little contribution from higher kaon resonances or nonresonant $J/\psi K3\pi$.

The optimized selection criteria for the $B^0 \to J/\psi K^0_S\pi^+\pi^-$ sample are $p_T(K^0_S) > 1.0$ GeV/c, $ct(B) > 30$ μm, and $I > 0.50$. This sample has less intrinsic background than the $B^0 \to J/\psi K^{*0}\pi^+\pi^-$ sample since the invariant mass peak of the K^0_S is narrower than that of the K^{*0} and its decay vertex is additionally displaced from the J/ψ decay vertex. To take advantage of this lower background, events that do not have enough SVX information to make a precise ct determination are included in a separate optimization which does not restrict $ct(B)$. The selection criteria for this sample are $p_T(K^0_S) > 1.9$ GeV/c and $I > 0.70$. These two samples are combined in Fig. 1(b). A fit yields 21.0 ± 6.3 signal candidates.

The signal width is fixed in the fit to $\sigma = 11.3$ MeV/c^2, based upon the expected width from the Monte Carlo simulation scaled up by the ratio of widths between the data and Monte Carlo for the reference mode $B^0 \to J/\psi K^0_S$. Allowing this width to float results in a fitted width which is approximately half the expected width. The excess of candidates at the B^0 mass is robust across a wide range of selection criteria and is broader when other selections are applied. The normalized mass distribution $(m_B - 5.28\ \text{GeV}/c^2)/\sigma_{m_B}$ has $\sigma = 0.67 \pm 0.21$ and 16.2 ± 5.6 candidates. The unusual narrowness appears to be primarily an artifact of this particular set of selection criteria which optimized the expected $S^2/(S + Bkg)$. Varying the signal Gaussian width by ±20% affects the fitted signal size by less than 2%.

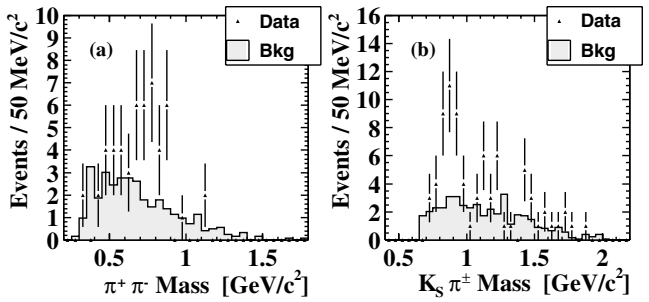

FIG. 2. $m(\pi^+\pi^-)$ (a) and $m(K^0_S\pi^\pm)$ (b) for $J/\psi K^0_S\pi^+\pi^-$ candidates within $\pm 2\sigma$ of the B^0 invariant mass.

The ratio of efficiencies, $R_\epsilon = 4.98$, combined with 84.1 ± 9.9 $B^0 \to J/\psi K^0_S$ reference candidates leads to a ratio of branching fractions of $\mathcal{B}(B^0 \to J/\psi K^0\pi^+\pi^-)/\mathcal{B}(B^0 \to J/\psi K^0) = 1.24 \pm 0.40$, where the error is statistical only. Using $\mathcal{B}(B^0 \to J/\psi K^0) = 8.3 \times 10^{-4}$ [6] leads to $\mathcal{B}(B^0 \to J/\psi K^0\pi^+\pi^-) = (10.3 \pm 3.3) \times 10^{-4}$.

Unlike $B^0 \to J/\psi K^{*0}\pi^+\pi^-$, $B^0 \to J/\psi K^0_S\pi^+\pi^-$ shows evidence of several substructure contributions in addition to $\psi(2S)K^0_S$ candidates. The $\pi^+\pi^-$ and $K^0_S\pi^\pm$ invariant mass plots shown in Fig. 2 have an excess of signal over background in the ρ^0 and $K^{*\pm}$ invariant mass regions, indicating possible contributions from $B^0 \to J/\psi K^0_S\rho^0$ and $B^0 \to J/\psi K^{*+}\pi^-$. The backgrounds are estimated from the $\pi^+\pi^-$ and $K^0_S\pi^\pm$ invariant mass distributions of the candidates in the B^0 mass sidebands.

To fit for these contributions, the B^0 invariant mass peaks for two samples of events are considered. Events in sample X have a $K^{*\pm} \to K^0_S\pi^\pm$ candidate with an invariant mass within 0.892 ± 0.051 GeV/c^2. Sample Y contains events which have a $\rho^0 \to \pi^+\pi^-$ candidate with an invariant mass within 0.770 ± 0.150 GeV/c^2 while excluding events in sample X. The $m(\pi^+\pi^-) > 0.55$ GeV/c^2 requirement is not placed upon sample X. Neither sample has any $\psi(2S)$ candidates. The invariant mass peaks of the B^0 candidates in these samples are fitted using a Gaussian signal of fixed width and a linear background. Figure 3 shows the results with sample X having 12.5 ± 4.6 fitted signal candidates and sample Y having 8.5 ± 3.8 fitted signal candidates.

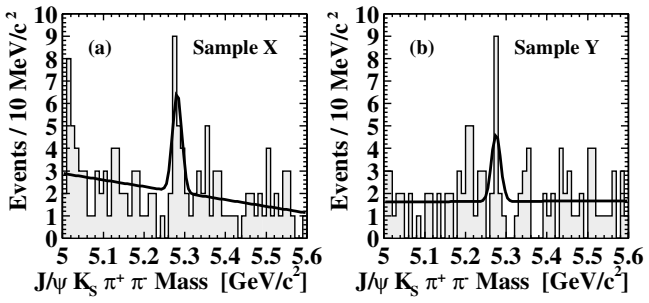

FIG. 3. B^0 candidate invariant masses for events with a $K^{*\pm}$ candidate (a) and those with a ρ^0 candidate but no $K^{*\pm}$ candidate (b).

Within $\pm 2\sigma$ of the B^0 mass, sample X has 21 candidates on a background of 9.2; sample Y has 14 candidates on a background of 7.3. These numbers of candidates lead to Feldman-Cousins 95% confidence intervals [7] for the signal size of $[4.1, 22.6]$ and $[1.1, 15.6]$ for samples X and Y, respectively. Using the fitted number of signal candidates and the efficiencies for $B^0 \to J/\psi K^0_S\rho^0$, $B^0 \to J/\psi K^{*+}\pi^-$, and $B^0 \to J/\psi K^0_S$ for each of the samples, the resulting branching fractions are $\mathcal{B}(B^0 \to J/\psi K^0\rho^0) = (5.4 \pm 2.9) \times 10^{-4}$ and $\mathcal{B}(B^0 \to J/\psi K^{*+}\pi^-) = (7.7 \pm 4.1) \times 10^{-4}$ with a correlation coefficient of -0.43. These branching fractions assume that these two modes are the dominant contributions to the two samples and that they do not interfere in the overlap region of their $K^0_S\pi^+\pi^-$ Dalitz plot.

The $J/\psi\pi^+\pi^-$ invariant mass plot of Fig. 4(a) shows 4 $\psi(2S)$ candidates on an expected background of 0.3. It is possible that $B^0 \to J/\psi K^0_S\rho^0$ and $J/\psi K^{*+}\pi^-$ come from $B^0 \to J/\psi K_1(1270)$. Figure 4(b) shows an excess in the $K^0_S\pi^+\pi^-$ invariant mass distribution near $K_1(1270)$, but there is also a small excess of candidates at higher $K^0_S\pi^+\pi^-$ invariant masses. The backgrounds are estimated from the $J/\psi\pi^+\pi^-$ and $K^0_S\pi^+\pi^-$ invariant mass distributions of the candidates in the B^0 invariant mass sidebands.

The results are summarized in Table I. The dominant uncertainty in these branching fractions is the statistical uncertainty due to the small signal size. Many of the systematic uncertainties cancel in the ratio of branching fractions with the reference mode. The systematic uncertainties that do not cancel to better than 2% are summarized in Table II and described as follows.

The signal modes have more helicity degrees of freedom than the reference modes, and the relative contributions of possible helicity states are not known. Varying the helicity composition in the Monte Carlo simulation introduces an uncertainty in the efficiencies of 9.9% for $J/\psi K^{*0}\pi^+\pi^-$ and 9.4% for $J/\psi K^0_S\pi^+\pi^-$. The uncertainty on the reference mode branching fraction does not enter into the ratio of branching fractions but it is a significant uncertainty for the branching fraction measurements. It is 8.3% for $J/\psi K^{*0}$ and 7.7% for $J/\psi K^0_S$. There is a 5%

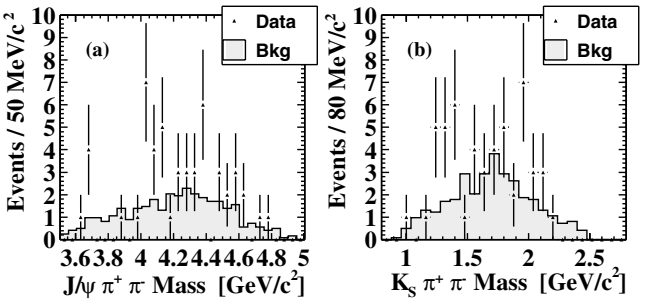

FIG. 4. $m(J/\psi\pi^+\pi^-)$ (a) and $m(K^0_S\pi^+\pi^-)$ (b) for $J/\psi K^0_S\pi^+\pi^-$ candidates within $\pm 2\sigma$ of the B^0 invariant mass.

TABLE I. Summary of results within $\pm 2\sigma$ of the B^0 invariant mass: Number of observed candidates ($N_{\rm obs}$); fitted background (Bkg); fitted signal ($S_{\rm fit}$); Feldman-Cousins 95% confidence interval on the signal size ($S_{\rm FC}$); fitted number of reference mode signal candidates ($S_{\rm ref}$); ratio of efficiencies (R_ϵ); and the branching fraction ($\mathcal{B}$) where the first uncertainty is statistical and the second is systematic.

	$J/\psi K^{*0}\pi^+\pi^-$	$J/\psi K^0\pi^+\pi^-$	$J/\psi K^0\rho^0$	$J/\psi K^{*+}\pi^-$
$N_{\rm obs}$	85	39	14	21
Bkg	54.0	21.1	7.32	9.22
$S_{\rm fit}$	36.3 ± 9.9	21.0 ± 6.3	8.5 ± 3.8	12.5 ± 4.6
$S_{\rm FC}$	[13.9, 50.8]	[7.1, 31.8]	[1.1, 15.6]	[4.2, 22.6]
$S_{\rm ref}$	257 ± 18	84.1 ± 9.9	84.1 ± 9.9	84.1 ± 9.9
R_ϵ	3.75	4.98	...	...
$\mathcal{B}/10^{-4}$	$6.6 \pm 1.9 \pm 1.1$	$10.3 \pm 3.3 \pm 1.5$	$5.4 \pm 2.9 \pm 0.9$	$7.7 \pm 4.1 \pm 1.3$

uncertainty in both signal modes due to uncertainties in the trigger model used in the Monte Carlo. Multiple decay modes could contribute to the final states studied here, but they all have similar reconstruction efficiencies. Varying the relative compositions in the Monte Carlo results in a net uncertainty of 5%. The effect of differing $p_T(B)$ spectra from various B production models introduces a 2.5% uncertainty. Uncertainty on the widths of the signal and background Gaussians in the $B^0 \to J/\psi K^{*0}\pi^+\pi^-$ sample results in a 7.5% uncertainty on the fitted signal size. The signal width uncertainty in the $B^0 \to J/\psi K_S^0\pi^+\pi^-$ sample contributes less than 2% uncertainty to the fitted signal size and thus is neglected. The $J/\psi K_S^0\rho^0$ and $J/\psi K^{*+}\pi^-$ branching fractions assume no interference in their overlap region in the $K_S^0\pi^+\pi^-$ Dalitz plot. Completely constructive interference would increase their combined branching fraction by $\sim$20%; a 10% systematic uncertainty is included in each mode to account for this possibility. Uncertainties on the reconstruction and vertexing efficiencies of the two extra signal pions are less than 2%.

The most statistically significant mode, $J/\psi K^{*0}\pi^+\pi^-$, has a significance of 3.7σ. $J/\psi K_S^0\pi^+\pi^-$ has a significance of 3.3σ; its submodes $J/\psi K_S^0\rho^0$ and $J/\psi K^{*+}\pi^-$ show hints of a signal but have less than 2σ significance.

TABLE II. Systematic uncertainties on $\mathcal{B}(B^0 \to J/\psi K^{(*)0}\pi^+\pi^-)$.

$\mathcal{B}(B^0 \to J/\psi K\pi^+\pi^-)$	% Uncertainty	
Source of uncertainty	$K = K^{*0}$	$K = K^0$
Helicity model	9.9	9.4
Reference mode $\mathcal{B}$	8.3	7.7
Signal width	7.5	...
Trigger model	5.0	5.0
Monte Carlo composition	5.0	5.0
B^0 production model	2.5	2.5
Combined uncertainties	17	14
Without ref. mode $\mathcal{B}$	15	12

We thank the Fermilab staff and the technical staffs of the participating institutions for their vital contributions. This research was supported by the U.S. Department of Energy and the National Science Foundation; the Italian Istituto Nazionale di Fisica Nucleare; the Ministry of Education, Science, Sports and Culture of Japan; the Natural Sciences and Engineering Research Council of Canada; the National Science Council of the Republic of China; the Swiss National Science Foundation; the A. P. Sloan Foundation; the Bundesministerium für Bildung und Forschung, Germany; the Korea Science and Engineering Foundation (KoSEF); the Korea Research Foundation; and the Comision Interministerial de Ciencia y Tecnologia, Spain.

*Present address: Northwestern University, Evanston, IL 60208.
†Present address: University of California, Santa Barbara, CA 93106.
‡Present address: Carnegie Mellon University, Pittsburgh, PA 15213.

[1] D. E. Groom *et al.,* Eur. Phys. J. C **15**, 1 (2000).
[2] A. Anastassov *et al.,* Phys. Rev. Lett. **84**, 1393 (2000).
[3] I. Dunietz *et al.,* Phys. Rev. D **43**, 2193 (1991).
[4] F. Abe *et al.,* Nucl. Instrum. Methods Phys. Res., Sect. A **271**, 387–403 (1988); D. Amidei *et al., ibid.* **350**, 73–130 (1994); F. Bedeschi *et al., ibid.* **268**, 50–74 (1988); G. Ascoli *et al., ibid.* **268**, 33–40 (1988).
[5] At CDF, the cylindrical axis of the CTC defines the z axis, which is aligned along the proton beam direction. ϕ is the azimuthal angle, θ is the polar angle, and r is the radial distance from the z axis. The pseudorapidity is defined as $\eta = -\ln[\tan(\theta/2)]$.
[6] B. Aubert *et al.,* Phys. Rev. D **65**, 032001 (2002).
[7] G. J. Feldman and R. D. Cousins, Phys. Rev. D **57**, 3873 (1998).